# Localization of the Kinesin-like Protein Xklp2 to Spindle Poles Requires a Leucine Zipper, a Microtubule-associated Protein, and Dynein

**Torsten Wittmann,* Haralabia Boleti,‡ Claude Antony,§ Eric Karsenti,* and Isabelle Vernos***

*European Molecular Biology Laboratory, Cell Biology and Cell Biophysics Programs, D-69117 Heidelberg, Germany; ‡Institut Pasteur, 75724 Paris Cedex 15, France; and §Institut Curie, 75248 Paris Cedex 05, France

***Abstract.*** Xklp2 is a plus end–directed *Xenopus* kinesin-like protein localized at spindle poles and required for centrosome separation during spindle assembly in *Xenopus* egg extracts. A glutathione-*S*-transferase fusion protein containing the COOH-terminal domain of Xklp2 (GST-Xklp2-Tail) was previously found to localize to spindle poles (Boleti, H., E. Karsenti, and I. Vernos. 1996. *Cell*. 84:49–59). Now, we have examined the mechanism of localization of GST-Xklp2-Tail. Immunofluorescence and electron microscopy showed that Xklp2 and GST-Xklp2-Tail localize specifically to the minus ends of spindle pole and aster microtubules in mitotic, but not in interphase, *Xenopus* egg extracts. We found that dimerization and a COOH-terminal leucine zipper are required for this localization: a single point mutation in the leucine zipper prevented targeting. The mechanism of localization is complex and two additional factors in mitotic egg extracts are required for the targeting of GST-Xklp2-Tail to microtubule minus ends: (*a*) a novel 100-kD microtubule-associated protein that we named TPX2 (Targeting protein for Xklp2) that mediates the binding of GST-Xklp2-Tail to microtubules and (*b*) the dynein–dynactin complex that is required for the accumulation of GST-Xklp2-Tail at microtubule minus ends. We propose two molecular mechanisms that could account for the localization of Xklp2 to microtubule minus ends.

Key words: kinesin-like protein • microtubule-associated protein • spindle • microtubule • dynein

During mitosis, chromosomes are segregated by a complex microtubule-based structure, the mitotic spindle. Current models of spindle assembly invoke the action of a variety of microtubule motors exerting forces on microtubules (reviewed in Barton and Goldstein, 1996; Hyman and Karsenti, 1996; Merdes and Cleveland, 1997; Vernos and Karsenti, 1996; Walczak and Mitchison, 1996). To understand how motors participate in spindle morphogenesis, we need to examine their function at different levels. One level concerns the mechanisms of motor localization through specific interactions between the variable nonmotor domains and their cargoes. For example, Nod, a kinesin-like protein (KLP)[1] associated with chromatin in *Drosophila* meiotic spindles, binds directly to DNA through a sequence homologous to the DNA-binding domain of HMG 14/17 (Afshar et al., 1995*a*, *b*). A second level deals with the actual motor function in relation to the activity of other plus and minus end–directed motors. For example, the BimC family KLPs, Kip1 and Cin8, counteract the activity of the minus end–directed COOH-terminal motor Kar3 in yeast (Hoyt et al., 1992; Saunders and Hoyt, 1992) and opposing motor activities have been implicated in the formation of mammalian spindle poles (Gaglio et al., 1996). A third level concerns the regulation of the activity and localization of motors in time and space by posttranslational modifications. For example, phosphorylation at specific cdc2 sites is required for the localization of human and *Xenopus* Eg5, a member of the BimC family, to spindle microtubules (Blangy et al., 1995; Sawin and Mitchison, 1995) and for the redistribution of the human KLP, CENP-E, from kinetochores to the spindle midzone during anaphase (Liao et al., 1994).

We recently reported that a *Xenopus* KLP, Xklp2, localizes to centrosomes and participates in their separation during mitosis (Boleti et al., 1996). A similar function has been proposed for motors of the BimC family (reviewed in Karsenti et al., 1996; Walczak and Mitchison, 1996; Kashina et al., 1997). Motors of the BimC family form bipolar

Address all correspondence to Isabelle Vernos, EMBL Heidelberg, Meyerhofstrasse 1, D-69117 Heidelberg, Germany. Tel.: 49 6221 387 324. Fax: 49 6221 387 306. E-mail: vernos@embl-heidelberg.de

1. *Abbreviations used in this paper*: GST, glutathione-*S*-transferase; KLP, kinesin-like protein; MAP, microtubule-associated protein; $T_m$, melting temperature; TPX2, Targeting protein for Xklp2.

tetramers suggesting that they may act by sliding antiparallel microtubules against each other (Kashina et al., 1996). Xklp2 was proposed to function in a different way. Motors tethered to one centrosome could move towards the plus end of microtubules emanating from the other, leading to their separation (Boleti et al., 1996; Karsenti et al., 1996). To better understand the role of Xklp2 in spindle pole separation we have examined in more detail the structural organization of Xklp2 and its mechanism of localization. We had previously reported (Boleti et al., 1996) that a GST-fusion protein containing the COOH-terminal domain of Xklp2 (amino acids 1137–1387; GST-Xklp2-Tail) was sufficient for its localization to spindle poles. Longer fragments including the tail showed the same localization, whereas the stalk domain alone (amino acids 363–1137) did not localize. Furthermore, only fusion proteins containing the tail and thus localizing to spindle poles had a dominant negative effect on spindle assembly pointing to the importance of this localization in Xklp2 function. Therefore, to understand how Xklp2 functions in centrosome separation, we have used GST-Xklp2-Tail to examine how Xklp2 is localized to spindle poles.

We now report that Xklp2 is a homodimer that localizes to the minus ends of microtubules rather than directly to centrosomes. This localization is cell cycle dependent, requires a COOH-terminal leucine zipper found in Xklp2, a novel microtubule-associated protein (MAP), and the activity of the dynein–dynactin complex.

## Materials and Methods

### Xenopus Egg Extracts

CSF-arrested extracts (mitotic extracts) were prepared according to Murray (1991). They were released to interphase by addition of 0.5 mM $CaCl_2$ and 200 μg/ml cycloheximide and subsequent incubation at 20°C for 45–60 min. High speed extracts were centrifuged for 60 min at 150,000 *g* at 4°C.

### Recombinant Proteins

The truncated Xklp2-Tail fragments were produced by PCR introducing BamHI and EcoRI restriction sites at their 5′- and 3′-ends, respectively, and cloned into a modified pGEX-2T vector (Pharmacia Biotech Sverige, Uppsala, Sweden). The construct GST-LtoK carrying a point mutation at amino acid 1370 was produced by overlap extension PCR with primers changing the codon CTG to AAG. All constructs were sequenced and did not contain mutations altering the amino acid sequence. The GST-fusion proteins were overexpressed in *E. coli* and purified by glutathione affinity chromatography using standard protocols. Subsequently the proteins were dialyzed against CSF-XB (10 mM K-Hepes, pH 7.7, 50 mM sucrose, 100 mM KCl, 2 mM $MgCl_2$, 0.1 mM $CaCl_2$, and 5 mM EGTA), frozen in liquid nitrogen and stored at −80°C.

### Antibodies

The anti-GST antibody was affinity purified against GST from a rabbit serum immunized with an unrelated GST-fusion protein. The anti-Xklp2-Tail antibody was an affinity-purified rabbit serum (Boleti et al., 1996) raised either against MBP- or GST-Xklp2-Tail fusion proteins. The anti-centrosome antibody was a human autoimmune serum strongly recognizing centrosomes in mammalian cells (Domínguez et al., 1994). The monoclonal m70.1 anti-dynein intermediate chain antibody was from Sigma Chemical Co. (St. Louis, MO). Fluorescent- and horseradish peroxidase–labeled antibodies were from Jackson ImmunoResearch Laboratories, Inc. (West Grove, PA).

### Localization Assay

Recombinant GST-Xklp2-Tail fusion proteins were added to 20 μl mitotic egg extract containing 0.2 mg/ml rhodamine-labeled tubulin (Hyman et al., 1991). Asters were assembled either by addition of human centrosomes purified from KE37 lymphoid cells as described (Bornens et al., 1987; Domínguez et al., 1994), 5% DMSO or 1 μM taxol (paclitaxel; Molecular Probes, Eugene, OR). The reactions were incubated for 30–60 min at 20°C, diluted with 1 ml BRB80 (80 mM K-PIPES, pH 6.8, 1 mM EGTA, and 1 mM $MgCl_2$) containing 10% glycerol, 0.25% glutaraldehyde, 1 mM GTP, and 0.1% Triton X-100 and subsequently centrifuged (HB4 rotor, 12,000 rpm, 12 min, 16°C) through a 25% glycerol cushion in BRB80 onto coverslips as described (Sawin and Mitchison, 1991). The coverslips were fixed in −20°C methanol, incubated twice for 10 min in 0.1% $NaBH_4$ in PBS and processed for immunofluorescence with the anti-GST-antibody. For immunolocalization with the anti-Xklp2-Tail antibody the dilution buffer did not contain glutaraldehyde but 5 μM taxol were included. All pictures were taken with Zeiss or Leica confocal microscopes. For biochemical analysis, asters were assembled in 150,000 g mitotic egg extracts with 1 μM taxol for 30 min at 20°C. The reactions were diluted 1:10 in BRB80 containing 5 mM EGTA, 0.1% Triton X-100, 1 mM DTT, protease inhibitors and 10 μg/ml cytochalasin D and spun through a 25% glycerol cushion in BRB80 (TLS-55 rotor, 20,000 rpm, 15 min, 20°C). The supernatant and pellet fractions were solubilized in SDS-PAGE sample buffer and analyzed by Western blotting.

### Electron Microscopy

Asters were assembled around human centrosomes, fixed with 1 ml BRB80 containing 0.25% glutaraldehyde, 1 mM GTP, and 0.1% Triton X-100, and spun onto polylysine-coated coverslips as for immunofluorescence. The coverslips were fixed for 10 min in the same buffer, rinsed in PBS, quenched for 30 min in 0.12% glycine in PBS and blocked for 15 min in 5% FCS in PBS. The coverslips were then incubated with the anti-GST antibody (2.5 μg/ml) in PBS, 5% FCS, 0.1% Triton X-100 for 45 min, washed with PBS, 1% FCS and stained with 10 nm protein A–gold (from J.W. Slot, Utrecht University, Utrecht, The Netherlands). After washing extensively with PBS, 1% FCS and once with PBS the samples were postfixed in 2% glutaraldehyde in PBS for 15 min, washed with 100 mM phosphate buffer, pH 7.2, and incubated for 15 min in 1.5% glutaraldehyde, 0.4% tannic acid in phosphate buffer. The samples were rinsed in phosphate buffer, treated with 0.5% $OsO_4$ in phosphate buffer for 10 min on ice, washed with water, stained with 1% uranyl acetate for 2 h at 4°C, dehydrated and flat embedded in Epon. After sectioning, the samples were contrasted with uranyl acetate and lead citrate and observed in a Philips CM120 electron microscope at 80 kV.

### Circular Dichroism Spectroscopy

GST-fusion proteins (~2 mg) were dialyzed against 150 mM Tris-HCl, pH 7.8, 150 mM NaCl, 5 mM $MgCl_2$, 2.5 mM $CaCl_2$, and 1 mM DTT and incubated with 10 units (3.2 μg) of thrombin (Sigma Chemical Co.) overnight at 4°C. The thrombin was removed by addition of 100 μl *p*-aminobenzamidine agarose (Sigma Chemical Co.) for 30 min on ice. Uncleaved protein and GST were removed by two subsequent incubations with 250 μl glutathione agarose for 30 min on ice. The proteins were dialyzed against 20 mM potassium phosphate pH 7.5, 20 mM KCl, 0.1 mM DTT, frozen in liquid nitrogen and stored at −80°C. The concentration of the cleaved proteins was determined with the BCA assay (Pierce Chemical Co., Rockford, IL). CD-spectra were recorded on a Jasco J-710 spectropolarimeter using cuvettes with 0.2- and 1-cm path length. Thermal unfolding was performed at a heating rate of 50 K/h and recorded at 0.2 K steps.

### Glutaraldehyde Cross-linking

2 μM Xklp2-Tail were incubated with varying concentrations of glutaraldehyde (Grade I; Sigma Chemical Co.) in 20 mM potassium phosphate pH 7.5, 20 mM KCl, 1 mM DTT for 30 min at 20°C. The reactions were stopped by the addition of one-half volume of 2 M glycine, mixed with SDS-PAGE sample buffer, and run on a 10% SDS-PAGE.

### Hydrodynamic Analysis

Mitotic or interphase egg extracts were centrifuged at 280,000 *g* for 20 min at 4°C. The Stokes radius of Xklp2 was determined by gel filtration chromatography of a 50-μl sample on a SMART Superose 6 column (Pharmacia Biotech Sverige) in CSF-XB. The sedimentation coefficient was estimated by sucrose gradient centrifugation. 100–200-μl samples were loaded on 4 ml 5–27% sucrose gradients in CSF-XB and spun for 16 h at

4°C at 27,000 rpm in a SW60 rotor. The elution profile of Xklp2 in both cases was determined by Western blotting of the fractions and probing with the anti-Xklp2-Tail antibody and compared with a variety of standard proteins of known Stokes radius and sedimentation coefficient, respectively. The standard proteins included rabbit muscle myosin (17.6 nm, 6.4 S), thyroglobulin (tetramer: 10.7 nm, 15 S, dimer: 6.7 nm, 12 S), γ-globulin (5.4 nm, 7.0 S), β-amylase (4.1 nm, 8.9 S), ovalbumin (2.8 nm, 3.5 S), catalase (11.3 S), aldolase (7.35 S), and BSA (4.6 S). The calculations were performed according to (Wilhelm et al., 1997).

### *Purification of TPX2*

CSF-arrested egg extract was diluted with two volumes of motor buffer (100 mM K-PIPES, pH 7.0, 0.5 mM EGTA, 2.5 mM magnesium acetate, and 1 mM DTT) containing 10 μg/ml pepstatin, leupeptin, aprotinin, and 1 mM PMSF, and then centrifuged for 90 min at 180,000 *g* at 4°C. The cytoplasmic layer was collected and supplemented with 0.6 mg/ml bovine brain tubulin (Ashford et al., 1998) and 20 μM taxol and microtubules were polymerized at room temperature for 30 min. The microtubules were then centrifuged through a 15% sucrose cushion in motor buffer (30,000 *g*, 20 min, 22°C). The supernatant was discarded, the cushion once washed with water, removed and the microtubule pellet resuspended in 1/3 of the original volume in motor buffer, and then centrifuged through a sucrose cushion again. MAPs were eluted in 100 mM steps of NaCl in motor buffer for 15 min at room temperature. Between the elution steps microtubules were recovered by centrifugation (30,000 *g*, 15 min, 22°C). TPX2 was enriched in the fraction eluted with 300 mM NaCl. This fraction was diluted to reduce the salt concentration and applied onto a PC 1.6/5 Mono S column (SMART system; Pharmacia Biotech Sverige). The column was eluted with a 1-ml linear gradient of 100–500 mM KCl in 20 mM K-PIPES, pH 7.0, 10% glycerol, 1 mM EDTA, 1 mM DTT, 0.01% Tween-20 at 4°C at 25 μl/min and 50-μl fractions were collected. TPX2 eluted at ~350 mM KCl. The peak fraction from the Mono S chromatography was applied to a PC 3.2/30 Superdex 200 gel filtration column (SMART system; Pharmacia Biotech Sverige) equilibrated with 20 mM K-Hepes, pH 7.0, 300 mM KCl, 10% glycerol, 1 mM EDTA, 1 mM DTT, and 0.01% Tween-20 at 4°C. The column was eluted with the same buffer at a flow rate of 20 μl/min and 40-μl fractions were collected. The column fractions were assayed in the following way: 4 mg/ml cycled bovine brain tubulin was polymerized in BRB80 containing 5 mM $MgCl_2$, 33% glycerol and 1 mM GTP at 37°C for 30 min. The microtubules were stabilized by the addition of 20 μM taxol. 5 μl MAPs or column fractions were mixed with 10 μl BRB80 containing 1 mM DTT, 5 μM taxol, 0.1% Triton X-100 and 1 μM GST-Xklp2-Tail. 5 μl of the prepolymerized microtubules were added and the reactions incubated at 20°C for 30 min. The reactions were then diluted 1:5 with BRB80 containing 1 mM DTT, 5 μM taxol, and 0.1% Triton X-100, and then centrifuged through a 10% sucrose cushion in BRB80, 5 μM taxol at 200,000 *g* at 20°C for 15 min. The cushion was washed once with water and the microtubule pellet solubilized in SDS-PAGE sample buffer and analyzed by Western blotting with the anti-GST antibody.

## *Results*

### *Cell Cycle–dependent Targeting of the COOH-terminal Domain of Xklp2 to Microtubule Minus Ends in Xenopus Egg Extracts*

We previously reported that Xklp2 is localized to centrosomes with a faint staining in interphase and a fairly strong staining at spindle poles. This suggested that there was a recruitment of Xklp2 at centrosomes (or spindle poles) during mitosis. To determine more precisely the localization of Xklp2 and its cell cycle dependence, we studied the targeting properties of a GST-fusion protein containing the COOH-terminal 250 amino acids of Xklp2 (GST-Xklp2-Tail) that localized to the poles of spindles formed around sperm nuclei in *Xenopus* egg extracts (Boleti et al., 1996). A simple localization assay was designed using microtubule asters formed in egg extracts by the addition of purified centrosomes. In extracts prepared from eggs naturally arrested in second metaphase of meiosis,

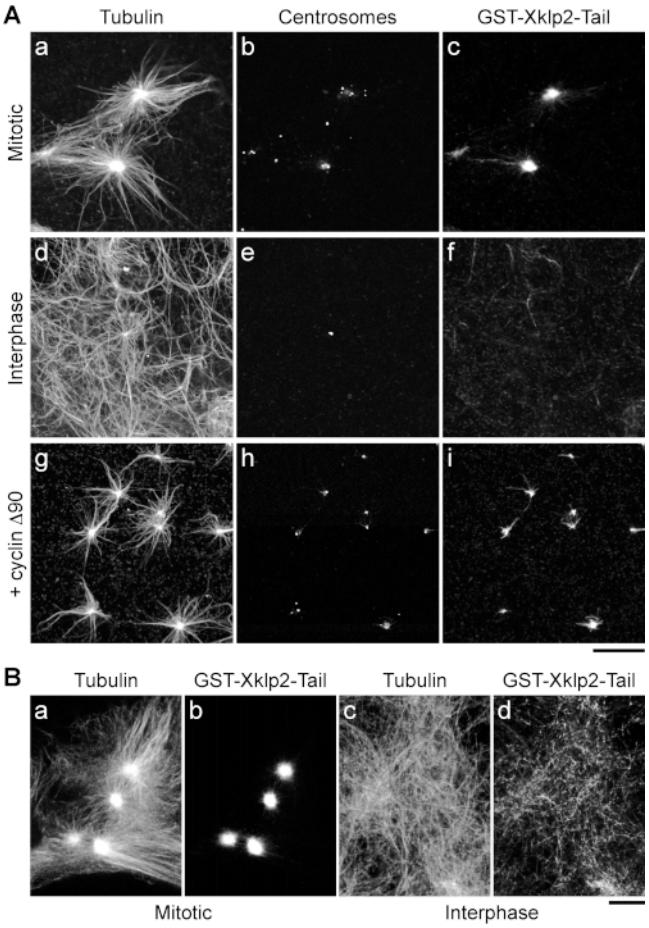


*Figure 1.* Localization of GST-Xklp2-Tail is cell cycle dependent. (*A*) Asters were assembled around human centrosomes in 10,000 g mitotic egg extract (*a–c*), the same extract released into interphase by the addition of calcium and cycloheximide (*d–f*), and cycled back to mitosis by addition of cyclin Δ90 (*g–i*). The asters were assembled in the presence of rhodaminated tubulin (*a*, *d*, and *g*), and stained with a human anti-centrosome antibody (*b*, *e*, and *h*), and an anti-GST antibody (*c*, *f*, and *i*) that were revealed with FITC- and Cy5-conjugated secondary antibodies, respectively. GST-Xklp2-Tail accumulates at the center of mitotic asters (*a–c*). This localization is abolished during interphase (*d–f*) and reappears after reentry into mitosis (*g–i*). (*B*) Asters assembled in the presence of 5% DMSO in 150,000 g mitotic egg extract (*a* and *b*), and microtubules in the same extract released to interphase before addition of DMSO (*c* and *d*). (*a* and *c*) Microtubules, (*b* and *d*) anti-GST-staining. GST-Xklp2-Tail is strongly concentrated at the center of mitotic DMSO asters (*b*) and stained diffusely along microtubules in interphase (*d*). All reactions contained 2 μM GST-Xklp2-Tail. Bars, 10 μm.

the GST-Xklp2-Tail protein accumulated in the center of the asters around the centrosomes (Figs. 1 *A*, *a–c* and 2, *A* and *G*). When the extract was released into interphase by addition of calcium, the microtubules formed an extended network and we did not observe any accumulation of the fusion protein anywhere in the sample and in particular, there was no enrichment of GST-Xklp2-Tail around centrosomes (Fig. 1 *A*, *d–f*). However, we observed a reproducible but very faint granular staining along a subset of

microtubules. This binding to microtubules was more obvious in high speed interphase extracts where microtubule polymerization was induced by addition of 5% DMSO. Under these conditions microtubules formed a disorganized network but did not form asters and the GST-Xklp2-Tail appeared to be spread along microtubules (Fig. 1 *B*, *d*). When the interphase extract was driven back into mitosis by addition of cyclin Δ90 (Glotzer et al., 1991), the GST-Xklp2-Tail was again observed strongly localized at the center of centrosome-nucleated asters (Fig. 1 *A*, *g–i*). These results indicated that the COOH-terminal domain of Xklp2 was sufficient to target Xklp2 to the center of microtubule asters specifically during mitosis. However, the apparent binding along microtubules in interphase extracts and the lack of association of GST-Xklp2-Tail with centrosomes in interphase raised the question of whether it was really interacting with centrosomes as indicated by our previous immunofluorescence results (Boleti et al., 1996).

To determine whether centrosomes were required for localization of the GST-Xklp2-Tail, asters and spindles were assembled in mitotic extracts in the absence of centrosomes (Stearns and Kirschner, 1994; Verde et al., 1991). The fusion protein localized efficiently to the center of asters assembled in the presence of 5% DMSO or 1 μM taxol in low speed (Fig. 2 *B*, *F*) or high speed mitotic extracts (Fig. 1 *B*, *b*) and to the poles of spindles assembled around DNA coated beads (Fig. 2 *C*; Heald et al., 1996). A fusion protein containing amino acids 363–1137, GST-Xklp2-Stalk, did not localize to the center of taxol-induced mitotic asters (Fig. 2 *E*) confirming that all the targeting information is contained in the GST-Xklp2-Tail construct. When the microtubules were depolymerized with nocodazole in centrosome-nucleated asters, the anti-GST-staining around the centrosomes disappeared completely (Fig. 2 *G*, *H*).

To test whether the endogenous Xklp2 was also recruited to the minus ends of microtubules in the absence of centrosomes, we performed immunofluorescence with an affinity-purified antibody raised against GST-Xklp2-Tail. This antibody strongly recognized Xklp2 on a Western blot of total egg extract (Fig. 2 *J*) and stained the center of asters assembled in the presence of 5% DMSO (Fig. 2 *K*). This result confirmed that Xklp2 is localized to the minus ends of microtubules rather than to the centrosomes themselves.

Immunogold electron microscopy of centrosomal asters assembled in mitotic egg extracts in the presence of the GST-Xklp2-Tail fusion protein also supported this idea. Staining with the anti-GST-antibody and protein A–gold revealed a strong accumulation of the protein on electron dense material along the minus ends of microtubules (Fig. 3 *A*), extending up to 1–2 μm away from the center of the aster. Gold particles were observed at a distance of up to 20–30 nm around the microtubules (note cross-sectioned microtubules, arrowheads in Fig. 3 *B*). Very few gold particles were found along microtubules further away from the center of the aster and the transition between the two areas was very sharp. In agreement with the immunofluorescence data presented above, no gold particles were found on the centrioles nor on the pericentriolar material itself (Fig. 3 *B*). No gold particles were found along mi-

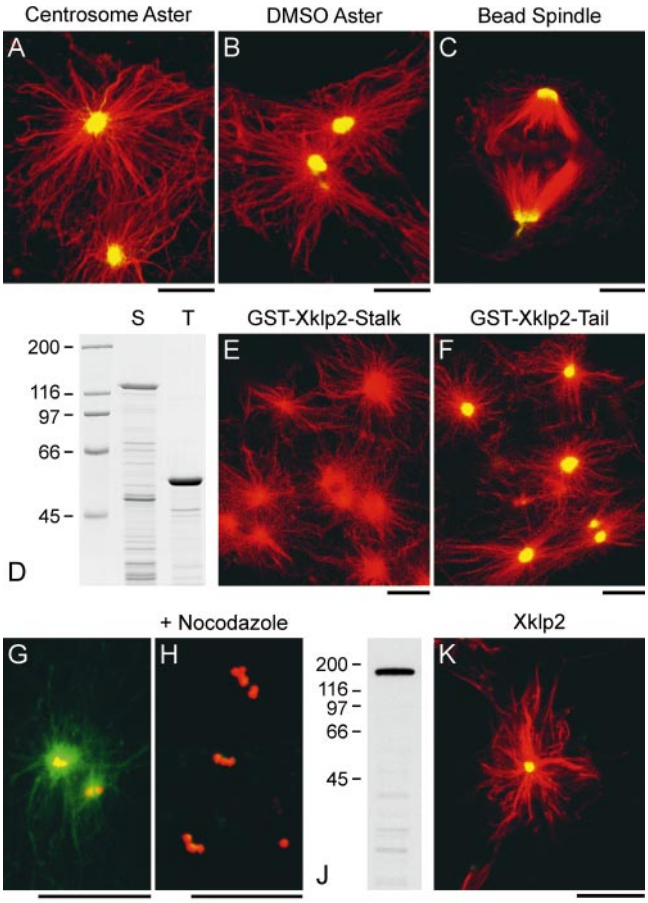


*Figure 2.* Both endogenous Xklp2 and GST-Xklp2-Tail localize to microtubule minus ends in mitotic asters in the absence of centrosomes. (*A–C*) Localization of GST-Xklp2-Tail. Microtubules are red, anti-GST-staining is green. (*A*) Aster nucleated by human centrosomes, (*B*) Aster assembled in the presence of 5% DMSO, (*C*) Spindle assembled around chromatin beads (Heald et al., 1996). Although there are no centrosomes present in *B* and *C*, GST-Xklp2-Tail accumulates at the center of the asters or the spindle poles, respectively. (*D–F*) The COOH-terminal domain of Xklp2 is necessary and sufficient for localization. (*D*) Coomassie-stained SDS-PAGE of GST-Xklp2-Stalk (amino acids 363–1137, *S*) and GST-Xklp2-Tail (amino acids 1137–1387, *T*). GST-Xklp2-Stalk does not localize to the center of taxol-induced mitotic asters (*E*) whereas GST-Xklp2-Tail does in a parallel experiment (*F*). (*G* and *H*) Depolymerization of microtubules eliminates GST-Xklp2-Tail staining around centrosomes. Centrosomes are red, anti-GST-staining is green, microtubules are not shown. (*G*) Aster nucleated by human centrosomes in the presence of 2 μM GST-Xklp2-Tail and stained with the human anti-centrosome antibody, (*H*) Asters assembled as in *G*, but treated with 5 μM nocodazole and incubated for 5 min on ice before fixation. (*J*) Western blot of 0.5 μl egg extract probed with an affinity-purified anti-Xklp2-Tail antibody. The antibody strongly recognizes a band of 160 kD. (*K*) Localization of the endogenous Xklp2. Microtubules are red, anti-Xklp2-staining is green. Asters were assembled with 5% DMSO in the presence of FITC-labeled tubulin and stained with the anti-Xklp2-Tail antibody (~5 μg/ml) and a Cy3-conjugated secondary antibody. The anti-Xklp2-Tail antibody stained the center of the DMSO-asters. Bars, 10 μm.

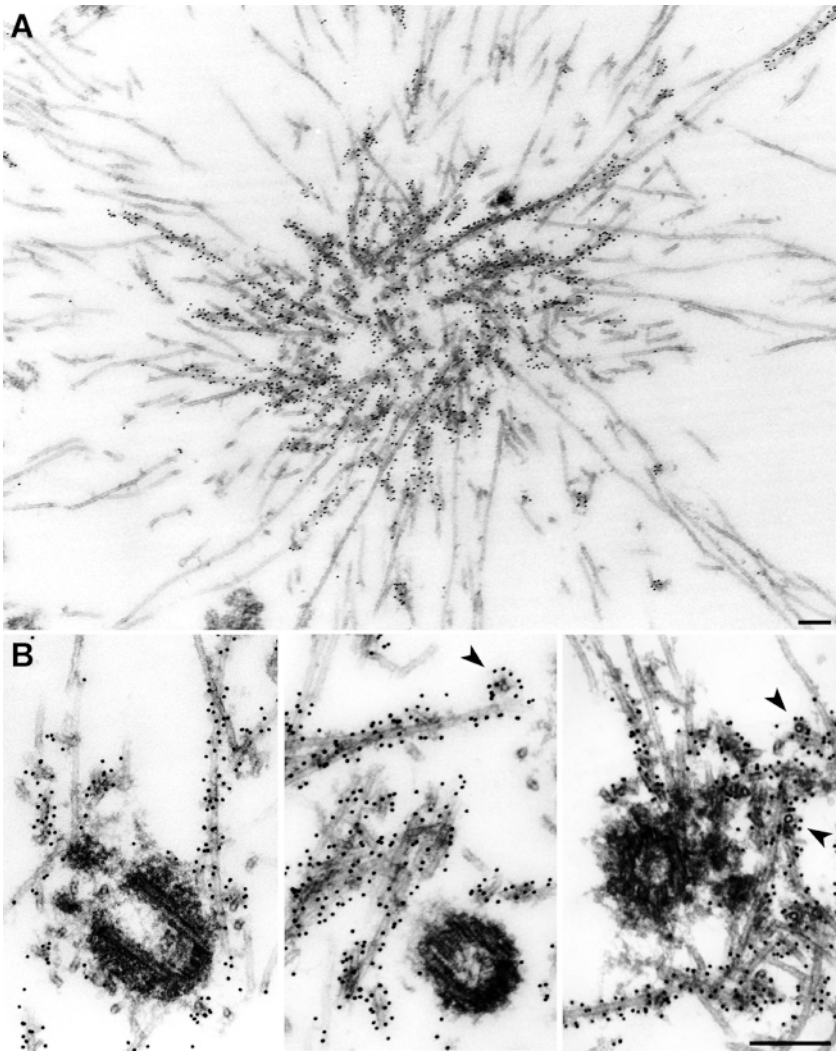


*Figure 3.* Localization of GST-Xklp2-Tail by immunoelectron microscopy. (*A*) Aster nucleated by purified human centrosomes in mitotic 10,000 g egg extract in the presence of 2 μM GST-Xklp2-Tail, stained with an anti-GST-antibody. The centrosomes are not visible in this section. (*B*) Centrosomes in the center of mitotic asters from the same sample. Gold particles were observed along microtubule minus ends but not on centrosomes. Arrowheads point to microtubules in cross-section, revealing the distance between gold particles and the microtubules. We did not observe any labeling in negative controls when the primary antibody was omitted or when the mutant fusion protein missing the leucine zipper (GST-Xklp2-CDel2) was added to the reaction instead of the tail (data not shown). Bars, 200 nm.

crotubules in negative control samples incubated with protein A–gold alone or with a mutant fusion protein that does not accumulate in the center of the asters (GST-Xklp2-CDel2, see below). These results indicate that Xklp2 is targeted to the minus ends of microtubules in a mitotic extract via its COOH-terminal domain. In interphase, the COOH-terminal domain of Xklp2 seems to bind weakly along the whole length of microtubules.

To confirm these results we compared the behavior of the COOH-terminal domain with that of the full-length endogenous Xklp2 protein using a biochemical analysis. Microtubules were assembled in the presence of 1 μM taxol in high speed mitotic and interphase egg extracts and sedimented by centrifugation through a glycerol cushion. A Coomassie-stained gel of the microtubule pellets showed that they contained mainly tubulin and a range of associated proteins (Fig. 4). Western blot analysis showed that ~5% of the total amount of Xklp2 (Fig. 4 *A*, lane *2*) was recovered in the mitotic microtubule pellet whereas a minor amount was detected in the interphase microtubule pellet and none at all in the absence of taxol (Fig. 4 *A*). Our previous biochemical analysis (Boleti et al., 1996) indicated that Xklp2 was released from microtubules by ATP. Since the assay was done in the presence of ATP, it reflected binding of Xklp2 to microtubules that was not due to its motor domain. The relatively low amount of Xklp2 that associates with microtubules under these conditions might be due to a low affinity of the ATP-independent binding site of Xklp2 for microtubules. This may lead to the dissociation of a significant amount of Xklp2 from microtubules during dilution of the extract and centrifugation of the microtubules through the cushion. When the GST-Xklp2-Tail fusion protein was present in the reactions at a concentration of 0.3 μM it behaved similarly to Xklp2 although it appeared to associate somewhat better with microtubules since ~10% of the fusion protein pelleted with mitotic microtubules (Fig. 4 *B*). Interestingly, under these conditions the amount of endogenous Xklp2 associated with the microtubule pellet was reduced indicating that the GST-Xklp2-Tail competed with the binding of the endogenous protein (Fig. 4 *B*, lane *2*). The GST-Xklp2-Tail also copelleted more efficiently than Xklp2 with interphase microtubules. The increased binding of GST-Xklp2-Tail to microtubules might be due to the fact that the construct was added in a slight molar excess (three- to

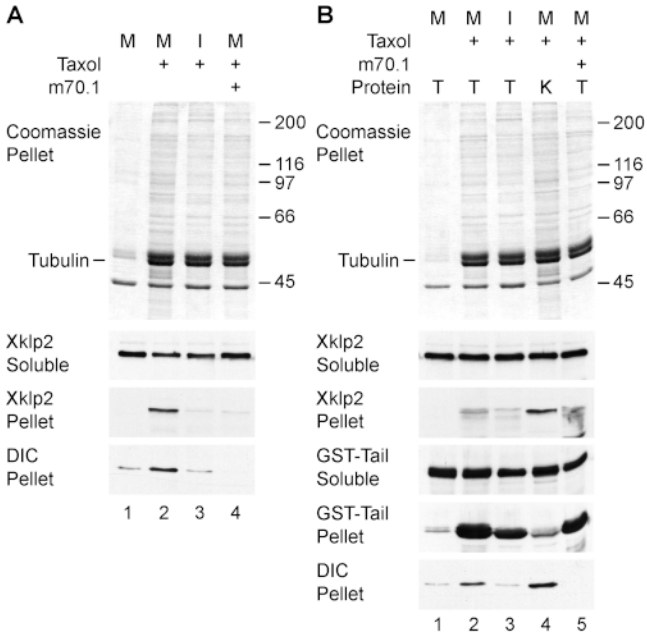


*Figure 4.* Biochemical analysis of Xklp2 cosedimentation with microtubules. Taxol (1 μM) and the m70.1 antibody (1–2 mg/ml) were added as indicated to 150,000 g egg extracts and the reactions incubated for 30 min at 20°C. *M*, mitotic extract, *I*, interphase extract. Microtubule pellets (corresponding to 5 μl of extract) and soluble fractions (corresponding to 0.25 μl of extract) were analyzed on Coomassie-stained gels and Western blots probed for the proteins indicated (*DIC*, dynein intermediate chain). (*A*) Sedimentation of endogenous Xklp2. (*B*) Sedimentation when either GST-Xklp2-Tail, *T*, or GST-Xklp2-LtoK, *K*, were added to the extract at 0.3 μM. Xklp2 as well as the GST-Xklp2-Tail sediment with microtubules in a mitotic cytoplasm. GST-Xklp2-Tail (52 kD) runs very close to the tubulin doublet. This is why the band on the Western blot of the microtubule pellet appears broadened. Also the dynein intermediate chain is enriched in mitotic microtubule pellets. When the m70.1 antibody is added the dynein intermediate chain is not associated with microtubules anymore and the binding of Xklp2 and GST-Xklp2-Tail to microtubules is reduced. The molecular mass of marker proteins is indicated on the right.

fivefold) over the endogenous protein. We conclude from these results that the GST-Xklp2-Tail has a similar behavior as the endogenous Xklp2 and is actively targeted to microtubule minus ends specifically during mitosis.

### *Targeting of Xklp2-Tail Requires Dimerization and a Leucine Zipper Domain*

To understand how the biophysical properties of Xklp2 could contribute to its localization and function, we first examined its quaternary structure. We determined its native molecular mass and hydrodynamic properties using gel filtration and sucrose gradient centrifugation. In both cases, Xklp2 behaved as a homogenous species. The results were identical for interphase and mitotic extracts within the experimental error. Therefore, we combined them to determine average values for the Stokes radius (10.4 ± 0.5 nm) and the sedimentation coefficient (8.1 ± 0.6 S). From these numbers we calculated a native molecular mass of 330 ± 40 kD, which is consistent with Xklp2 being an homodimer (the calculated molecular mass for an Xklp2 homodimer is 320 kD). In addition, these data indicated that Xklp2 is a highly asymmetric molecule with an approximate axial ratio of 20, as one would expect for a rod-shaped protein containing a fairly long (~1,000 amino acids) coiled-coil domain.

To examine whether a leucine zipper that we had previously identified at the COOH-terminal end of Xklp2 (Boleti et al., 1996) was important for localization, we prepared a series of GST-fusion proteins which truncated the tail domain either at the $NH_2$- or at the COOH-terminal ends (Fig. 5, *A* and *B*). Asters were assembled in mitotic egg extracts in the presence of 2 μM of the corresponding fusion protein and their localization was determined by immunofluorescence with an anti-GST antibody. The same results were obtained in the three conditions tested: on asters nucleated by human centrosomes in low speed extracts, on DMSO-asters generated in high speed extracts (Fig. 5 *C*) and on half spindles assembled around *Xenopus* sperm nuclei (data not shown). With the $NH_2$-terminal deletion series we observed a gradual decrease in localization efficiency as estimated from the fluorescence intensity of the anti-GST staining: GST-NDel1 was localized with ~40% efficiency compared with GST-Xklp2-Tail whereas GST-NDel2 was not visible on centrosomal asters and weakly on DMSO-asters (probably reflecting the higher microtubule density in this later case). GST-NDel3, which contains only the leucine zipper, did not show any localization at all. The first deletion from the COOH-terminal end, GST-CDel1, missing the last five amino acids (not involved in coiled-coil interactions) localized as efficiently as GST-Xklp2-Tail. GST-CDel2 that lacks the entire leucine zipper (33 amino acids) was not targeted at all. To determine whether the leucine zipper structure was required for the localization, we introduced a charged amino acid into its hydrophobic core. In this mutant, GST-LtoK, the leucine 1370 was changed to a lysine. This protein was not localized in any of the three conditions tested. In addition, GST-LtoK did not cosediment significantly with mitotic microtubules and did not compete with the binding of the endogenous Xklp2 (Fig. 4 *B*, lane *4*). These results showed that the leucine zipper is essential but not sufficient for localization to the center of mitotic asters and that some regions $NH_2$-terminal to it were also required.

Since the $NH_2$-terminal region of the Xklp2-Tail was predicted to have the highest coiled-coil forming potential (Fig. 5 *A*) apart from the leucine zipper itself, we examined whether dimerization was important for localization. We first determined the oligomeric state of the Xklp2-Tail by chemical cross-linking. This technique had been used previously to characterize coiled-coil interactions (Frère et al., 1995; Harborth et al., 1995). Xklp2-Tail from which the GST had been removed by thrombin treatment was incubated with increasing concentrations of glutaraldehyde and analyzed by SDS–gel electrophoresis (Fig. 6 *A*). At the highest glutaraldehyde concentration the 32-kD band corresponding to the monomer disappeared completely and was replaced by a single other band of ~60 kD. This strongly suggests that Xklp2-Tail mainly exists as a dimer in solution. The lack of reaction products of higher apparent molecular mass suggested that the cross-linking was

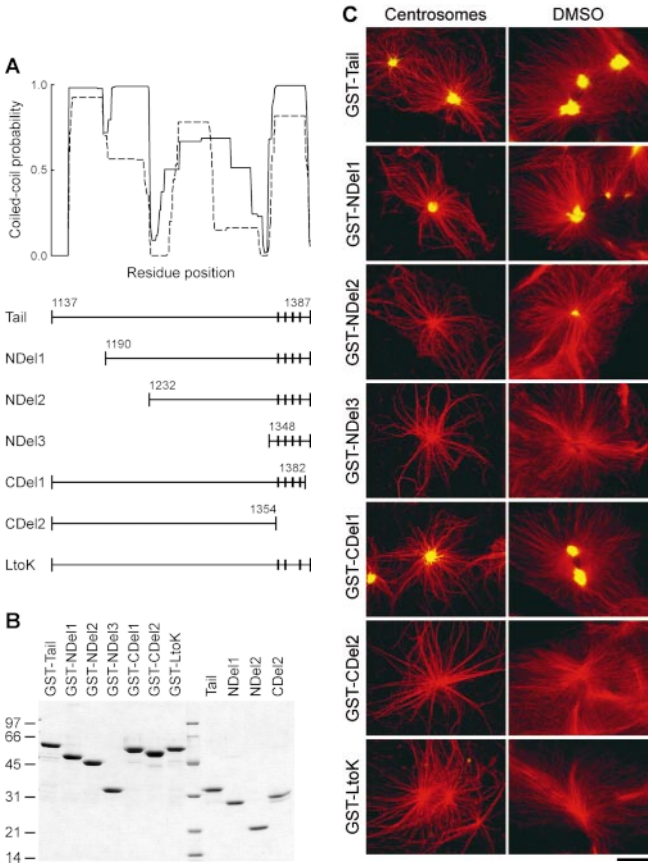


*Figure 5.* Localization of the truncated GST-Xklp2-Tail fusion proteins to mitotic asters. (*A*) Coiled-coil prediction for the Xklp2-Tail obtained with the Coils- (*solid line*; Lupas et al., 1991) and the Paircoil-algorithm (*dashed line*; Berger et al., 1995), and schematic representation of the different constructs. Vertical bars represent the four leucines present in the leucine zipper. (*B*) Coomassie Brilliant blue–stained SDS-gel of the purified GST-fusion proteins and the thrombin-cleaved proteins used for circular dichroism spectroscopy. The molecular mass of marker proteins is indicated on the left. (*C*) Localization of the GST-fusion proteins to asters nucleated by human centrosomes in 10,000 g egg extract and to DMSO-asters in 150,000 g egg extract. The fusion proteins were added at a concentration of 2 μM and are indicated on the left. Both the $NH_2$-terminal region and the COOH-terminal leucine zipper are required for localization of the GST-Xklp2-Tail to the center of mitotic asters. Microtubules are red, anti-GST-staining is green. Bar, 10 μm.

specific. Cross-linking with formaldehyde was less efficient but yielded similar results (data not shown).

We then determined the respective role of the $NH_2$-terminal region and the leucine zipper in stable dimerization. Far UV circular dichroism spectroscopy showed that Xklp2-Tail as well as NDel2 and CDel2 are mainly α-helical at a concentration of 2 μM (Fig. 6 *B*). The helical content was estimated to be ~80% according to the method described by Zhong and Johnson (1992). Furthermore, the ratio $[\theta]_{222}/[\theta]_{208}$ was close to 1.0 for all three fragments suggesting a coiled-coil conformation (Lau et al., 1984).

To examine the relative stability of the different fragments, we monitored the thermal unfolding at 222 nm (Fig. 6 *C*). At a concentration of 10 μM, Xklp2-Tail had a melting temperature ($T_m$) of ~40°C. Deletion of the leucine zipper, CDel2, did not affect the stability of the protein severely, whereas deletions of the $NH_2$-terminal coiled-coil domain, NDel1 and NDel2, clearly lowered $T_m$. Therefore, the $NH_2$-terminal sequences are essential for dimer stability. This was further confirmed by looking at the concentration dependence of $T_m$ for the different constructs. A 10-fold dilution of Xklp2-Tail or of CDel2 did not affect their $T_m$ significantly, indicating a very strong dimerization, whereas a 10-fold dilution of NDel2 significantly lowered its $T_m$ indicating a weakened dimerization (Fig. 6 *D*). The presence of GST had no effect on the stability of the dimeric Xklp2-Tail moiety (Fig. 6 *E*). The melting curves of GST-Xklp2-Tail and Xklp2-Tail were overlapping in the region where the melting of Xklp2-Tail occurred. The GST-moiety denatured irreversibly at higher temperature (above 50°C). The same was observed for other fusion proteins tested (data not shown) indicating that the results obtained by circular dichroism reflected the differential localization of the fusion proteins in the extract.

Taken together these data show that both dimerization of Xklp2 and the COOH-terminal leucine zipper are essential for its targeting to microtubule minus ends.

### *Targeting of Xklp2-Tail to Microtubule Minus Ends Requires a Functional Dynein–Dynactin Complex*

Next, we wanted to understand how Xklp2 could be localized to microtubule minus ends. This was not due to its own motor activity since the GST-Xklp2-Tail has no motor domain and, furthermore, Xklp2 is a plus end–directed motor. NuMA, a protein associated with mitotic spindle poles, has been shown to form a complex with cytoplasmic dynein and dynactin and to be recruited to the spindle poles in a dynein dependent way (Gaglio et al., 1996; Merdes et al., 1996). We therefore tested whether dynein could also transport Xklp2 towards microtubule minus ends. We used the monoclonal antibody m70.1 directed against the dynein intermediate chain to inhibit dynein function in egg extracts (Steuer et al., 1990; Heald et al., 1996; Gaglio et al., 1997).

Using the microtubule aster sedimentation assay described above, we determined by Western blot analysis that the dynein intermediate chain was enriched in the microtubule pellets from mitotic extract (Fig. 4 *A*, lane *2*, and *B*, lanes *2* and *4*). Addition of the m70.1 antibody to the extract reduced the level of dynein intermediate chain in the microtubule pellet to a nondetectable level (Fig. 4 *A*, lane *4*, and *B*, lane *5*), supporting the idea that this antibody disrupts the interaction of the dynein intermediate and heavy chains with spindle microtubules (Heald et al., 1997). Under these conditions, almost no endogenous Xklp2 was found in the microtubule pellet (Fig. 4 *A*, lane *4*) whereas the binding of the GST-Xklp2-Tail was only slightly reduced (Fig. 4 *B*, lane *5*). Again, this difference might be due to a difference in affinity for microtubules between the full-length protein and the tail construct or to the slight molar excess of GST-Xklp2-Tail added to the extract. In any case, these results indicated that inhibition of the interaction between dynein and microtubules af-

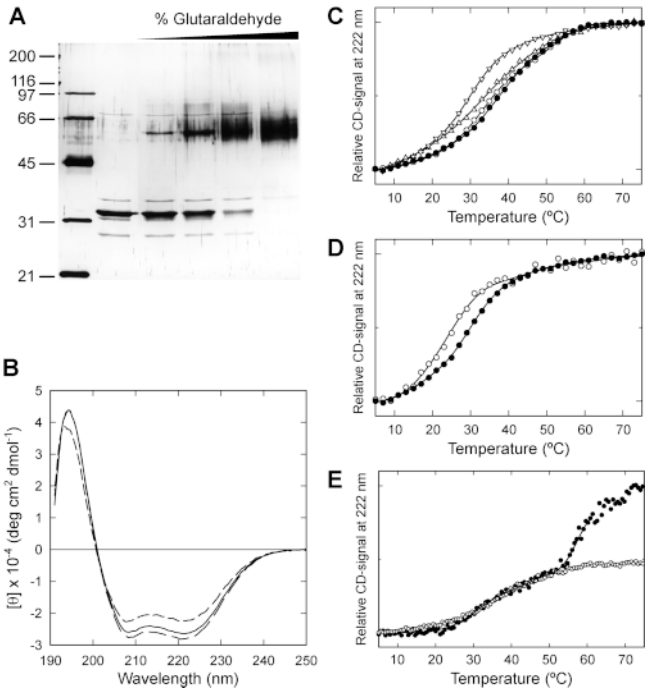


*Figure 6.* Dimerization of the Xklp2-Tail. (*A*) Silver-stained SDS-PAGE of thrombin-cleaved Xklp2-Tail incubated with increasing amounts of glutaraldehyde (from left to right: markers, 0, 0.0003, 0.001, 0.003, and 0.01%). With rising glutaraldehyde concentrations, a new band appears at 60 kD corresponding to the dimeric Xklp2-Tail. The molecular mass of marker proteins is indicated on the left. (*B*) Far UV circular dichroism spectra of Xklp2-Tail (*solid line*), CDel2 (*long dash*), and NDel2 (*short dash*) at 2 μM concentration at 4°C. (*C*) Thermal unfolding of Xklp2-Tail (*filled circle*), CDel2 (*open circle*), NDel1 (*triangle*), NDel2 (*upsidedown triangle*) at 10 μM. (*D*) Thermal unfolding of Xklp2-NDel2 at a concentration of 10 μM (*filled circle*) and 1 μM (*open circle*). (*E*) Thermal unfolding of GST-Xklp2-Tail (*filled circle*) and Xklp2-Tail (*open circle*) at 10 μM concentration. See text for details.

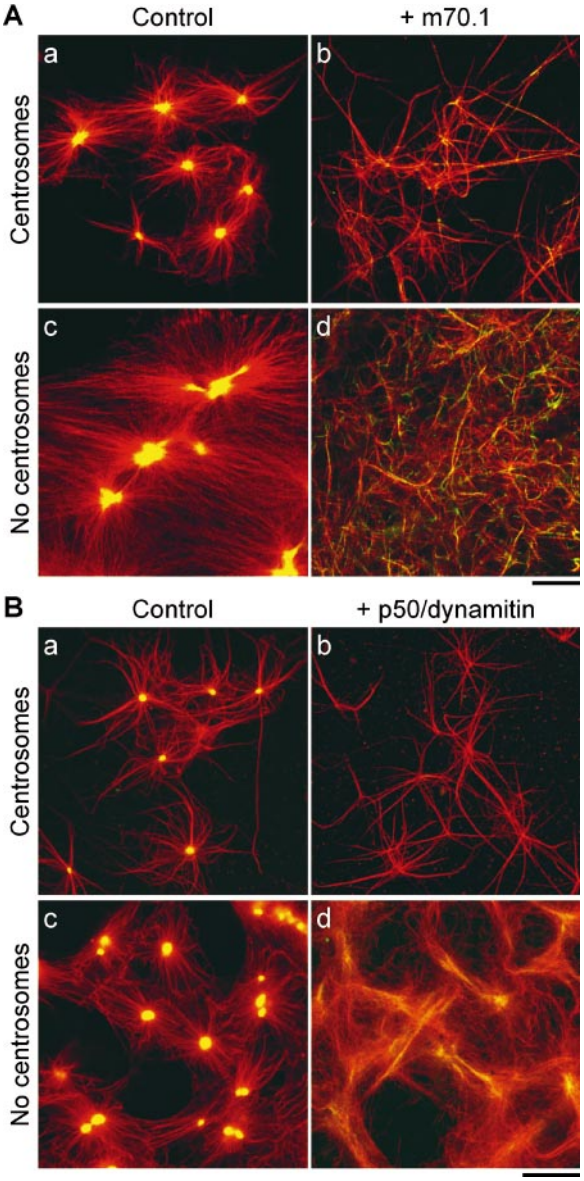


*Figure 7.* Cytoplasmic dynein and the dynactin complex are required for localization of GST-Xklp2-Tail. (*A*) Human centrosomes were added to 10,000 g mitotic egg extract and incubated at 20°C. After 10 min, 1–2 mg/ml m70.1 antibody was added to *b*, after another 5 min 2 μM GST-Xklp2-Tail was added and the reaction incubated for 45 min. (*d*) 1–2 mg/ml m70.1 was added to 150,000 g egg extract and incubated for 5 min on ice. Microtubule polymerization was then induced by addition of 5% DMSO and incubation for 30 min at 20°C. In both cases addition of m70.1 disrupts the localization of GST-Xklp2-Tail to the center of mitotic asters. (*B*) Disruption of the dynactin complex inhibits localization of GST-Xklp2-Tail. (*b*) Asters nucleated by human centrosomes in the presence of partially purified bacterially expressed p50/dynamitin (~1 mg/ml) in 10,000 g mitotic egg extract for 60 min at 20°C. (*d*) Asters assembled by 1 μM taxol in the presence of 1 mg/ml p50/dynamitin in 10,000 g mitotic egg extract for 30 min at 20°C. Microtubules are red, anti-GST-staining is green. Bars, 10 μm.

fected the binding of Xklp2 to microtubules in some way but did not address whether it affected its targeting to microtubule minus ends.

To examine the effect of dynein inhibition on the localization of GST-Xklp2-Tail on microtubule asters, centrosome-nucleated asters were assembled in the presence of the m70.1 antibody. Although some microtubules appeared to be bundled and detached from the centrosomes, asters could still be detected reasonably well. Under these conditions, the localization of GST-Xklp2-Tail to the center of the asters was severely reduced, but a very weak staining was observed along microtubule bundles (Fig. 7 *A*, *b*). The m70.1 antibody blocked more dramatically the formation of asters in mitotic extracts treated with 5% DMSO or taxol as predicted by previous studies on dynein dependence of aster formation in the absence of centrosomes (Verde et al., 1991). Again, the GST-Xklp2-Tail was found spread along microtubules (Fig. 7 *A*, *d*) indicating that dynein function was required for the accumulation of Xklp2 to microtubule minus ends in mitotic asters. It also showed that when dynein function was blocked in the

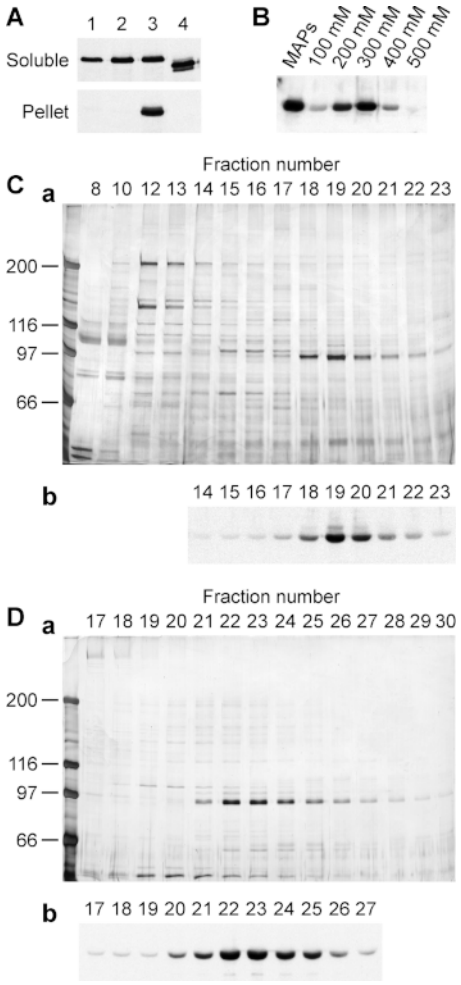


*Figure 8.* Purification of TPX2, a MAP that mediates the binding of Xklp2 to microtubules. (*A*) GST-Xklp2-Tail alone does not bind to pure taxol-stabilized microtubules (lane *1*). However, a fraction of MAPs contains an activity that mediates the binding of GST-Xklp2-Tail to microtubules (lane *3*). This activity was assayed in the following way: lane *1*, prepolymerized microtubules were mixed with either GST-Xklp2-Tail and control buffer; lane *2*, GST-Xklp2-Tail and soluble proteins (0.6 mg/ml) from CSF-arrested egg extract; lane *3*, GST-Xklp2-Tail and MAPs (0.6 mg/ml); lane *4*, or GST-Xklp2-CDel2 and MAPs. The microtubules were sedimented by centrifugation through a sucrose cushion and the soluble fractions and pellets (four times more loaded than of the soluble fraction) were analyzed by Western blotting, probed with an anti-GST antibody. (*B*) Fractionation of MAPs by sequential salt elution from microtubules. Microtubules polymerized in CSF-arrested egg extract were purified by centrifugation through a sucrose cushion and eluted in one step with 500 mM NaCl (MAPs) or sequentially with the NaCl concentration indicated. The fractions were assayed as described above and the pellets were analyzed by Western blotting and probed with an anti-GST antibody. (*C*) Mono S chromatography of the 300 mM NaCl fraction eluted from microtubules. (*a*) Silver-stained SDS-PAGE of 5-μl aliquots of the fractions indicated. The molecular mass of marker proteins is indicated on the left. (*b*) Assay for the activity mediating the binding of GST-Xklp2-Tail to microtubules of fractions from the Mono S chromatography as indicated. (*D*) The peak fraction of the Mono S chromatography was applied to a Superdex 200 gel filtration column. (*a*) Silver-stained gel of 5-μl aliquots of the fractions indicated. (*b*) Assay for the activity mediating the binding of GST-Xklp2-Tail to microtubules of fractions from the Superdex 200 gel filtration chromatography as indicated. In both chromatographic steps the activity copurified with a 100-kD protein.

presence of the m70.1 antibody the GST-Xklp2-Tail could still bind all along microtubules.

We then examined if the dynactin complex was also involved in Xklp2-Tail localization to microtubule minus ends. Overexpression of the p50/dynamitin protein in tissue culture cells has been shown to disrupt the dynactin complex (Echeverri et al., 1996). Addition of bacterially expressed and partially purified p50/dynamitin to *Xenopus* egg extracts resulted in the reduction of the sedimentation velocity of the $p150^{Glued}$ subunit of dynactin indicating that the complex had dissociated (Wittmann and Hyman, 1999) as previously reported for tissue culture cells (Echeverri et al., 1996). In the presence of p50/dynamitin, centrosomes still nucleated asters that looked similar to those generated in the presence of the m70.1 antibody. Again, this abolished the localization of the GST-Xklp2-Tail to the center of the asters (Fig. 7 *B*, *b*). When microtubule polymerization was induced by the addition of taxol in the presence of p50/dynamitin the asters were highly disorganized and GST-Xklp2-Tail failed to localize (Fig. 7 *B*, *d*). Also in the presence of p50/dynamitin we could observe a significant binding of GST-Xklp2-Tail along microtubules. Altogether these results show that cytoplasmic dynein as well as the dynactin complex are required for the localization of GST-Xklp2-Tail to microtubule minus ends during mitosis. Interestingly in the absence of dynein function, GST-Xklp2-Tail could still bind all along microtubules although with a lower efficiency as determined biochemically.

### *Binding of Xklp2-Tail to Microtubules Requires TPX2, a Novel 100-kD MAP*

The above set of experiments suggested that the targeting of Xklp2-Tail to microtubule minus ends occurred in two steps: (*a*) binding to microtubules and (*b*) localization to microtubule minus ends through the action of the dynein–dynactin complex. Although dynein could mediate the interaction between endogenous Xklp2 and microtubules in some way it could not be responsible for microtubule binding since even in the presence of dynein inhibitors we still detected binding of GST-Xklp2-Tail to microtubules both biochemically and by immunofluorescence (see Fig. 4 *B*, lane *5* and Fig. 7). Moreover, we could not detect any interaction between dynein or dynactin and Xklp2 or GST-Xklp2-Tail in immunoprecipitation experiments (data not shown).

We then wanted to test whether the GST-Xklp2-Tail itself contained a microtubule-binding activity using a biochemical assay. Pure taxol-stabilized microtubules were mixed with the GST-Xklp2-Tail and the microtubules were then sedimented by centrifugation through a sucrose cushion and analyzed by Western blot. Under these conditions, no GST-Xklp2-Tail was detected in the microtubule pellet (Fig. 8 *A*, lane *1*). To determine whether an additional protein was required for GST-Xklp2-Tail binding to microtubules, we prepared MAPs from CSF-arrested egg

extract. Identical amounts of either the proteins that remained soluble or MAPs were included in the reaction (Fig. 8 *A*, lanes *2* and *3*, respectively). Only in the presence of the MAP-fraction a substantial amount of GST-Xklp2-Tail was recovered in the microtubule pellet. We observed by immunofluorescence that in this case GST-Xklp2-Tail bound all along the prepolymerized microtubules showing no preference for either end (data not shown). The fusion protein lacking the leucine zipper, GST-Xklp2-CDel2, did not cosediment with MAPs and microtubules demonstrating the specificity of the assay (Fig. 8 *A*, lane *4*). These results indicated the presence of a factor in mitotic egg extracts required for the binding of the COOH-terminal domain of Xklp2 to microtubules that was enriched in a MAP-fraction prepared from CSF-arrested egg extract.

Affinity chromatography of total extracts or MAPs passed over a GST-Xklp2-Tail protein column did not yield any interacting proteins (data not shown). Therefore, we attempted the purification of the factor mediating the binding of GST-Xklp2-Tail to microtubules using classical biochemistry. As a first purification step, mitotic MAPs were eluted from microtubules with steps of 100 mM NaCl and the different fractions were tested whether they could promote GST-Xklp2-Tail binding to microtubules (Fig. 8 *B*). Most of the targeting factor remained bound to microtubules up to a salt concentration of 200 mM but was eluted by 300 mM salt. This protein fraction was then applied to a Mono S column and eluted with a linear salt gradient. The activity that mediated the binding of GST-Xklp2-Tail to microtubules eluted from the Mono S column in a single peak at around 350 mM KCl and corresponded to a doublet of polypeptides with molecular masses of ~100 kD (Fig. 8 *C*). The strong affinity of these proteins for the Mono S suggested that they were highly basic. Since the Mono S peak fraction still contained some minor contaminants it was further purified on a Superdex 200 gel filtration column (Fig. 8 *D*). Also on this column the activity mediating the binding of GST-Xklp2-Tail copurified with the 100-kD band. The peaks of minor contaminating bands left after the Mono S did not coelute with the activity. These results showed that a MAP that we named TPX2 (Targeting Protein for Xklp2), mediated the binding of the COOH-terminal domain of Xklp2 to microtubules. Purified TPX2 itself was able to rebind to pure microtubules (data not shown). Interestingly, the Xklp2-Tail carrying a single point mutation in the leucine zipper (GST-LtoK) did not bind at all to microtubules in the presence of this MAP. This strongly suggests that TPX2 is the receptor for the leucine zipper found at the COOH terminus of Xklp2.

## Discussion

### *Xklp2 Accumulates at Microtubule Minus Ends during Mitosis*

We have previously shown that Xklp2 is required for centrosome separation. This function is shared with other motors like those of the BimC family. At first sight, both Xklp2 and the *Xenopus* member of the BimC family, Eg5, had a similar localization at spindle poles and even on centrosomes (Sawin et al., 1992; Boleti et al., 1996). A more careful examination of this localization revealed that Eg5 is actually distributed throughout the spindle (Sawin and Mitchison, 1995). On the basis of initial immunofluorescence results we also reported that Xklp2 was on centrosomes. Here, we have clearly established that at least a fraction of Xklp2 and the recombinant GST-Xklp2-Tail do not bind to centrosomes directly. They are rather localized to the minus ends of microtubules in mitosis and at least a fraction appears to bind all over the microtubule length in interphase. Our earlier conclusion was based on the fact that some staining remained associated with centrosomes after depolymerization of microtubules by nocodazole in XL177 tissue culture cells (Boleti et al., 1996). However, there are alternative explanations for this observation, e.g., incomplete disassembly of microtubules close to the centrosome. In any case, the important result as far as Xklp2 function in centrosome separation is concerned is that it is localized close to microtubule minus ends during mitosis. Interestingly, a similar discrepancy has been observed for the localization of the microtubule-severing ATPase katanin. Katanin is localized to the centrosomal area and its localization has been reported to be microtubule dependent in sea urchin embryos (McNally et al., 1996) whereas the centrosomal localization in tissue culture cells was not affected by microtubule depolymerization (Hartman et al., 1998).

The structural organization and localization of Xklp2 indicates that its mechanism of action is different from Eg5 and probably complements it. Eg5 belongs to the BimC family that form bipolar tetramers with motor domains on both ends (reviewed by Kashina et al., 1997). Tetrameric Eg5 moves towards the plus ends of microtubules while simultaneously bundling and sorting them into antiparallel arrays. Xklp2 is proposed to function as a dimer concentrated at microtubule minus ends which separates the poles by exerting a plus end–directed force on microtubules emanating from the opposite pole (Boleti et al., 1996). The difference between the two motors is mainly the site where the force is produced and it is likely that both functions are essential to establish spindle bipolarity and to stabilize the bipolar shape. This is why the inactivation of any of these plus end–directed motors gives an apparently similar phenotype whereas their specific function in defining spindle shape is entirely different. The function of Xklp2 may be mostly to help the initiation of centrosome separation in the initial phases of spindle assembly. This is consistent with a recent study showing that inhibition of Xklp2 has little effect on spindles assembled in the absence of centrosomes around chromatin beads (Walczak et al., 1998).

### *Mechanism of Xklp2 Localization to Microtubule Minus Ends*

Although we still do not understand very well how KLPs are localized to their different sites of action within the cell, it is generally accepted that regions in the nonconserved nonmotor domains of KLPs confer targeting specificity (reviewed by Goldstein, 1993). KLPs could be attached to their target in two different ways: through a direct interaction as it has been determined for Nod, a chromatin bound KLP, that has been shown to interact di-

rectly with DNA via an 82–amino acid region in its COOH-terminal domain (Afshar et al., 1995*b*); or through a complex with other proteins such as the binding of kinesin to vesicles, which involves kinectin, an integral membrane protein that anchors kinesin to the surface of membrane vesicles (Kumar et al., 1995; reviewed in Vallee and Sheetz, 1996).

The targeting of Xklp2 to microtubule minus ends is complex and seems to involve several steps. To dissect this mechanism, we have used the COOH-terminal domain of Xklp2 that was shown to be necessary and sufficient to target the protein to spindle poles.

***Targeting of Xklp2 to Microtubules by TPX2.*** We have identified TPX2, a 100-kD MAP, that is required to mediate the binding of Xklp2 to microtubules. However, TPX2 is not sufficient to localize Xklp2 to microtubule minus ends. Most MAPs have been identified by their ability to bind microtubules and for some of them the effect on microtubule dynamics has been studied (e.g., Andersen and Karsenti, 1997). Only few examples are known of MAPs that link other cellular components to microtubules. It has been suggested that $p34^{cdc2}$ kinase associates with microtubules in the mitotic spindle because of its interaction with MAP4 (Ookata et al., 1995). CLIP-170 has been characterized as a cytoplasmic linker protein that mediates the binding of endocytic vesicles to microtubules (Pierre et al., 1992). A similar brain-specific protein, CLIP-115, links dendritic lamellar bodies to microtubules (De Zeeuw et al., 1997). Both CLIPs share a homologous microtubule binding motif with $p150^{Glued}$, a component of the dynactin complex, that has also been shown to bind directly to microtubules (Waterman-Storer et al., 1995). NuMA has been shown to bind both microtubules and the dynein–dynactin complex (Merdes et al., 1996). Cytoplasmic dynein binds through its intermediate chain to $p150^{Glued}$ (Karki and Holzbaur, 1995). Interestingly, human Eg5 seems to interact also with $p150^{Glued}$ (Blangy et al., 1997). To our knowledge TPX2 represents the only other example of a MAP that binds directly to a KLP. The microtubule localization of the yeast KLP Kar3 is dependent on its interaction with Cik1 (Page et al., 1994), but since Cik1 does not show a microtubule binding activity on its own it is more similar to a kinesin light chain than to a MAP.

Our data show that a very COOH-terminal leucine zipper is required for the interaction between TPX2 and Xklp2, whereas the more $NH_2$-terminal regions of the Xklp2 COOH-terminal domain are required for the stability of the dimeric structure. This dimerization is also required for Xklp2 targeting. Therefore, the COOH-terminal domain of Xklp2 interacts through its leucine zipper with TPX2 that mediates the binding of Xklp2 to microtubules. It is interesting to note that Xklp2 does not seem to bind to TPX2 in the absence of microtubules. Since Xklp2 does not bind either to microtubules in the absence of TPX2, it seems that the stable binding of Xklp2 to microtubules involves a ternary complex between microtubules, TPX2 and the tail of Xklp2. Why dimerization of the tail is required is not yet understood. Because of the apparent weak interaction between Xklp2 and microtubules in the extract (GST-Xklp2-Tail can inhibit the endogenous protein in equimolar amounts, see Boleti et al., 1996), we think that this dimerization is important to stabilize the ternary complex on the microtubules. The weak interaction between Xklp2 and TPX2/microtubules may also account for the apparent differences in binding properties of the GST-Xklp2-Tail and the endogenous protein. We usually add an excess of GST-Xklp2-Tail to our assays and this seems to be sufficient to increase the binding efficiency of the tail relative to the endogenous protein to microtubules.

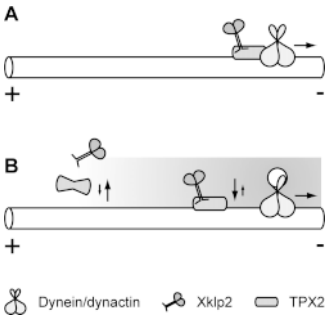


*Figure 9.* Two alternative models for how Xklp2 and TPX2 could be localized to microtubule minus ends in a dynein dependent way. (*A*) Direct mechanism: Xklp2 and TPX2 interact with a dynein containing complex that moves towards the microtubule minus end or they bind directly to a component that has been transported there by dynein before. (*B*) Indirect mechanism: a protein that is transported to the minus ends by dynein creates a gradient along the microtubule (possibly by some enzymatic activity) that changes the affinity of TPX2 to Xklp2 and/or to microtubules.

***Localization of Xklp2 to the Minus Ends by Dynein.*** Our data indicate that the targeting of Xklp2 to microtubule minus ends involves the dynein–dynactin complex. Cytoplasmic dynein, a minus end–directed motor, and the dynactin complex, a modulator of cytoplasmic dynein function, are localized to spindle poles and required for the generation and maintenance of focused poles (Steuer et al., 1990; Paschal et al., 1993; Echeverri et al., 1996; Heald et al., 1996, 1997). Moreover, cytoplasmic dynein is required for the movement of exogenously added microtubule seeds to the minus end of microtubules, suggesting that it is involved in the transport of microtubules towards the spindle poles. In addition, other proteins are localized to spindle poles in a dynein dependent manner. NuMA, a coiled-coil protein that cross-links microtubules at the spindle poles, has been shown to interact directly with dynactin and cytoplasmic dynein (Merdes et al., 1996) and appears to be displaced at least partially when dynein function is inhibited (Gaglio et al., 1996; Heald et al., 1997).

We found that the localization of GST-Xklp2-Tail to microtubule minus ends was disrupted by interfering with either dynein using the m70.1 antibody or dynactin by addition of p50/dynamitin to the extract. Since the m70.1 antibody dissociates both the dynein intermediate and heavy chains from spindle microtubules (Gaglio et al., 1997; Heald et al., 1997) the present findings demonstrate that dynein is required for the localization of Xklp2 to microtubule minus ends.

Therefore, we are left with two findings: a MAP, TPX2, mediates the binding of Xklp2 to microtubules and the dynein–dynactin complex is required to bring Xklp2 to the minus end of microtubules. We can think of two different mechanisms leading to Xklp2 localization at microtubule

minus ends: (*a*) a direct mechanism in which Xklp2 and TPX2 may be part of a larger complex containing dynein/dynactin, NuMA and maybe other proteins that are moved towards the spindle poles by the motor activity of dynein (Fig. 9 *A*). Xklp2 and TPX2 could also be recruited to the pole by binding to components that have been transported there by dynein already, but this would still involve a series of direct interactions between Xklp2 and TPX2 on one side and dynein–dynactin on the other; (*b*) an indirect mechanism in which an enzymatic activity (e.g., a protein kinase or phosphatase) is transported towards microtubule minus ends by dynein. Because in an aster, dynein accumulates at microtubule minus ends, this could create a gradient of enzymatic activity along the microtubules of the aster. This could, in turn, increase the affinity of Xklp2 and TPX2 for each other and/or for microtubules close to the microtubule minus end (Fig. 9 *B*).

From our present data we can not distinguish between these two possibilities and further work will be necessary to clarify how certain proteins are enriched at a specific end of a microtubule. It is interesting to note that in interphase or in mitotic extracts in which dynein has been inactivated Xklp2 binds along microtubules. This suggests that the cell cycle regulation of Xklp2 localization to microtubule minus ends may involve a specific function of dynein during mitosis.

In any case, this work has unraveled a very interesting mechanism where a minus end–directed motor, dynein, can organize spindle poles and at the same time participates in the localization of a plus end–directed motor to the poles, an event required for their separation: this is another example of how several levels of self-organizing processes can lead to the assembly of a machine as complex as a mitotic spindle.

We would like to thank L. Serrano for his invaluable help with the circular dichroism spectroscopy and S. Reinsch, R. Heald, J. Domínguez, T. Hyman, and M. Glotzer for advice and gifts of reagents. We also thank N. Le Bot, A. Westerholm, R. Tournebize, and S. Andersen for critical reading of the manuscript.

Received for publication 23 February 1998 and in revised form 9 September 1998.

### *References*

Afshar, K., N.R. Barton, R.S. Hawley, and L.S. Goldstein. 1995*a*. DNA binding and meiotic chromosomal localization of the *Drosophila* nod kinesin-like protein. *Cell*. 81:129–138.

Afshar, K., J. Scholey, and R.S. Hawley. 1995*b*. Identification of the chromosome localization domain of the *Drosophila* Nod kinesin-like protein. *J. Cell Biol.* 131:833–843.

Andersen, S.S.L., and E. Karsenti. 1997. XMAP310: A *Xenopus* rescue-promoting factor localized to the mitotic spindle. *J. Cell Biol.* 139:975–983.

Ashford, A.J., S.S.L. Andersen, and A.A. Hyman. 1998. Preparation of tubulin from bovine brain. *In* Cell Biology: A Laboratory Handbook. Vol. 2. J.E. Celis, editor. Academic Press, San Diego, CA. 205–212.

Barton, N.R., and L.S.B. Goldstein. 1996. Going mobile: microtubule motors and chromosome segregation. *Proc. Natl. Acad. Sci. USA*. 93:1735–1742.

Berger, B., D.B. Wilson, E. Wolf, T. Tonchev, M. Milla, and P.S. Kim. 1995. Predicting coiled coils by use of pairwise residue correlations. *Proc. Natl. Acad. Sci. USA*. 92:8259–8263.

Blangy, A., H.A. Lane, P. d'Herin, M. Harper, M. Kress, and E.A. Nigg. 1995. Phosphorylation by $p34^{cdc2}$ regulates spindle association of human Eg5, a kinesin-related motor essential for bipolar spindle formation in vivo. *Cell*. 83: 1159–1169.

Blangy, A., L. Arnaud, and E.A. Nigg. 1997. Phosphorylation by $p34^{cdc2}$ protein kinase regulates binding of the kinesin-related motor HsEg5 to the dynactin subunit $p150^{Glued}$. *J. Biol. Chem.* 272:19418–19424.

Boleti, H., E. Karsenti, and I. Vernos. 1996. Xklp2, a novel Xenopus centrosomal kinesin-like protein required for centrosome separation during mitosis. *Cell*. 84:49–59.

Bornens, M., M. Paintrand, J. Berges, M.C. Marty, and E. Karsenti. 1987. Structural and chemical characterization of isolated centrosomes. *Cell Motil. Cytoskel.* 8:238–249.

De Zeeuw, C.I., C.C. Hoogenraad, E. Goedknegt, E. Hertzberg, A. Neubauer, F. Grosveld, and N. Galjart. 1997. CLIP-115, a novel brain-specific cytoplasmic linker protein, mediates the localization of dendritic lamellar bodies. *Neuron*. 19:1187–1199.

Domínguez, J.E., B. Buendia, C. Lopez-Otin, C. Antony, E. Karsenti, and J. Avila. 1994. A protein related to brain microtubule-associated protein MAP1B is a component of the mammalian centrosome. *J. Cell Sci.* 107:601–611.

Echeverri, C.J., B.M. Paschal, K.T. Vaughan, and R.B. Vallee. 1996. Molecular characterization of the 50-kD subunit of dynactin reveals function for the complex in chromosome alignment and spindle organization during mitosis. *J. Cell Biol.* 132:617–633.

Frère, V., F. Sourgen, M. Monnot, F. Troalen, and S. Fermandjian. 1995. A peptide fragment of human DNA topoisomerase II alpha forms a stable coiled-coil structure in solution. *J. Biol. Chem.* 270:17502–17507.

Gaglio, T., A. Saredi, J.B. Bingham, M.J. Hasbani, S.R. Gill, T.A. Schroer, and D.A. Compton. 1996. Opposing motor activities are required for the organization of the mammalian mitotic spindle pole. *J. Cell Biol.* 135:399–414.

Gaglio, T., M.A. Dionne, and D.A. Compton. 1997. Mitotic spindle poles are organized by structural and motor proteins in addition to centrosom *J. Cell Biol.* 138:1055–1066.

Glotzer, M., A.W. Murray, and M.W. Kirschner. 1991. Cyclin is degraded by the ubiquitin pathway. *Nature*. 349:132–138.

Goldstein, L.S.B. 1993. With apologies to Scheherazade: tails of 1001 kinesin motors. *Annu. Rev. Genet.* 27:319–351.

Harborth, J., K. Weber, and M. Osborn. 1995. Epitope mapping and direct visualization of the parallel, in-register arrangement of the double-stranded coiled-coil in the NuMA protein. *EMBO J.* 14:2447–2460.

Hartman, J.J., J. Mahr, K. McNally, K. Okawa, A. Iwamatsu, S. Thomas, S. Cheesman, J. Heuser, R.D. Vale, and F.J. McNally. 1998. Katanin, a microtubule-severing protein, is a novel AAA ATPase that targets to the centrosome using a WD40-containing subunit. *Cell*. 93:277–287.

Heald, R., R. Tournebize, T. Blank, R. Sandaltzopoulos, P. Becker, A. Hyman, and E. Karsenti. 1996. Self-organization of microtubules into bipolar spindles around artificial chromosomes in *Xenopus* egg extracts. *Nature*. 382: 420–425.

Heald, R., R. Tournebize, A. Habermann, E. Karsenti, and A. Hyman. 1997. Spindle assembly in *Xenopus* egg extracts: Respective roles of centrosomes and microtubule self-organization. *J. Cell Biol.* 138:615–628.

Hoyt, M.A., L. He, K.K. Loo, and W.S. Saunders. 1992. Two *Saccharomyces cerevisiae* kinesin-related gene products required for mitotic spindle assembly. *J. Cell Biol.* 118:109–120.

Hyman, A.A., and E. Karsenti. 1996. Morphogenetic properties of microtubules and mitotic spindle assembly. *Cell*. 84:401–410.

Hyman, A.A., D. Drechsel, D. Kellogg, S. Salser, K. Sawin, P. Steffen, L. Wordeman, and T.J. Mitchison. 1991. Preparation of modified tubulins. *In* Methods in Enzymology. Vol. 196. R.B. Vallee, editor. Academic Press, San Diego, CA. 478–485.

Karki, S., and E.L.F. Holzbaur. 1995. Affinity chromatography demonstrates a direct binding between cytoplasmic dynein and the dynactin complex. *J. Biol. Chem.* 270:28806–28811.

Karsenti, E., H. Boleti, and I. Vernos. 1996. The role of microtubule dependent motors in centrosome movements and spindle pole organization during mitosis. *Sem. Cell Biol.* 7:367–378.

Kashina, A.S., R.J. Baskin, D.G. Cole, K.P. Wedaman, W.M. Saxton, and J.M. Scholey. 1996. A bipolar kinesin. *Nature*. 379:270–272.

Kashina, A.S., G.C. Rogers, and J.M. Scholey. 1997. The bimC family of kinesins: essential bipolar mitotic motors driving centrosome separation. *Biochim. Biophys. Acta*. 1357:257–271.

Kumar, J., H. Yu, and M.P. Sheetz. 1995. Kinectin, an essential anchor for kinesin-driven vesicle motility. *Science*. 267:1834–1837.

Lau, S.Y.M., A.K. Taneja, and S.H. Hodges. 1984. Synthesis of a model protein of defined secondary and quaternary structure. *J. Biol. Chem.* 259:13253–13261.

Liao, H., G. Li, and T.J. Yen. 1994. Mitotic regulation of microtubule cross-linking activity of CENP-E kinetochore protein. *Science*. 265:394–398.

Lupas, A., M. van Dyke, and J. Stock. 1991. Predicting coiled coils from protein sequences. *Science*. 252:1162–1164.

McNally, F.J., K. Okawa, A. Iwamatsu, and R.D. Vale. 1996. Katanin, the microtubule-severing ATPase, is concentrated at centrosomes. *J. Cell. Sci.* 109: 561–567.

Merdes, A., and D.W. Cleveland. 1997. Pathways of spindle pole formation: different mechanisms; conserved components. *J. Cell Biol.* 138:953–956.

Merdes, A., K. Ramyar, J.D. Vechio, and D.W. Cleveland. 1996. A complex of NuMA and cytoplasmic dynein is essential for spindle assembly. *Cell*. 87: 447–458.

Murray, A.W. 1991. Cell cycle extracts. *In* Methods in Cell Biology. Vol. 36. B.K. Kay and H.B. Peng, editors. Academic Press, San Diego, CA. 581–605.

Ookata, K., S. Hisanaga, J.C. Bulinski, H. Murofushi, H. Aizawa, T.J. Itoh, H. Hotani, E. Okumura, K. Tachibana, and T. Kishimoto. 1995. Cyclin B interaction with microtubule-associated protein 4 (MAP4) targets $p34^{cdc2}$ kinase

to microtubules and is a potential regulator of M-phase microtubule dynamics. *J. Cell Biol.* 128:849–862.

Page, B.D., L.L. Satterwhite, M.D. Rose, and M. Snyder. 1994. Localization of the Kar3 kinesin heavy chain-related protein requires the Cik1 interacting protein. *J. Cell Biol.* 124:507–519.

Paschal, B.M., E.L.F. Holzbaur, K.K. Pfister, S. Clark, D.I. Meyer, and R.B. Vallee. 1993. Characterization of a 50-kDa polypeptide in cytoplasmic dynein preparations reveals a complex with $p150^{Glued}$ and a novel actin. *J. Biol. Chem.* 268:15318–15323.

Pierre, P., J. Scheel, J.E. Rickard, and T.E. Kreis. 1992. CLIP-170 links endocytic vesicles to microtubules. *Cell*. 70:887–900.

Saunders, W.S., and M.A. Hoyt. 1992. Kinesin-related proteins required for structural integrity of the mitotic spindle. *Cell*. 70:451–458.

Sawin, K.E., and T.J. Mitchison. 1991. Mitotic spindle assembly by two different pathways in vitro. *J. Cell Biol.* 112:925–940.

Sawin, K.E., and T.J. Mitchison. 1995. Mutations in the kinesin-like protein Eg5 disrupting localization to the mitotic spindle. *Proc. Natl. Acad. Sci. USA*. 92: 4289–4293.

Sawin, K.E., K. LeGuellec, M. Philippe, and T.J. Mitchison. 1992. Mitotic spindle organization by a plus-end-directed microtubule motor. *Nature*. 359: 540–543.

Stearns, T., and M. Kirschner. 1994. In vitro reconstitution of centrosome assembly and function: the central role of γ-tubulin. *Cell*. 76:623–637.

Steuer, E.R., L. Wordeman, T.A. Schroer, and M.P. Sheetz. 1990. Localization of cytoplasmic dynein to mitotic spindles and kinetochores. *Nature*. 345:266–268.

Vallee, R.B., and M.P. Sheetz. 1996. Targeting of motor proteins. *Science*. 271: 1539–1544.

Verde, F., J.M. Berrez, C. Antony, and E. Karsenti. 1991. Taxol-induced microtubule asters in mitotic extracts of *Xenopus* eggs: requirement for phosphorylated factors and cytoplasmic dynein. *J. Cell Biol.* 112:1177–1187.

Vernos, I., and E. Karsenti. 1996. Motors involved in spindle assembly and chromosome segregation. *Curr. Opin. Cell Biol.* 8:4–9.

Walczak, C.E., and T.J. Mitchison. 1996. Kinesin-related proteins at mitotic spindle poles: function and regulation. *Cell*. 85:943–946.

Walczak, C.E., I. Vernos, T.J. Mitchison, E. Karsenti, and R. Heald. 1998. A model for the proposed roles of different microtubule-based motor proteins in establishing spindle bipolarity. *Curr. Biol.* 8:903–913.

Waterman-Storer, C.M., S. Karki, and E.L.F. Holzbaur. 1995. The $p150^{Glued}$ component of the dynactin complex binds to both microtubules and the actin-related protein centractin (Arp-1). *Proc. Natl. Acad. Sci. USA*. 92:1634–1638.

Wilhelm, H., S.S.L. Andersen, and E. Karsenti. 1997. Purification of recombinant cyclin B1/cdc2 kinase from Xenopus egg extracts. *In* Methods in Enzymology. Vol. 283. W.G. Dunphy, editor. Academic Press, San Diego, CA. 12–28.

Wittmann, T., and T. Hyman. 1999. Recombinant p50/dynamitin as a tool to examine the role of dynactin in intracellular processes. *In* Methods in Cell Biology. Vol. 61. C. Rieder, editor. Academic Press, San Diego, CA. 137–143.

Zhong, L., and W.C. Johnson. 1992. Environment affects amino acid preference for secondary structure. *Proc. Natl. Acad. Sci. USA*. 89:4462–4465.